

A METHOD TO EVALUATE THE PERFORMANCE OF X-RAY IMAGING SCINTILLATORS BY MEANS OF THE BRIGHTNESS-SHARPNESS INDEX (BSI)

D. CAVOURAS¹, I. KANDARAKIS¹, P. PRASSOPOULOS², E. KANELLOPOULOS¹, C. D. NOMICOS³ and G. S. PANAYIOTAKIS⁴

¹Department of Medical Instrumentation Technology, Technological Educational Institution of Athens, Athens, ²Department of Radiology, University Hospital, Medical School, University of Crete, Heraklion, ³Department of Electronics, Technological Educational Institution of Athens, Athens, and ⁴Department of Medical Physics, Medical School, University of Patras, Patras, Greece.

Abstract

Purpose: To propose an image quality index, the brightness-sharpness index (BSI), for assessing the quality of the image produced by phosphors of medical imaging detectors.

Material and Methods: BSI was evaluated by experimental X-ray luminescence and modulation transfer function measurements. BSI was determined for a number of test phosphor screens prepared from Gd₂O₂S:Tb, La₂O₂S:Tb, and Y₂O₂S:Tb phosphor materials. The screens covered a wide range of coating thicknesses from 50 to 150 mg/cm² and measurements were performed for X-ray tube voltages between 50 and 120 kVp.

Results: Gd₂O₂S:Tb phosphor exhibited higher brightness and sharpness, as compared to the other phosphor materials, for all screens and X-ray tube voltages used. Best Gd₂O₂S:Tb performance was observed for thin screens and high tube voltages. La₂O₂S:Tb exhibited higher BSI values than Y₂O₂S:Tb for medium and high tube voltages.

Conclusion: Results showed that phosphor materials of high X-ray detection and X-ray-to-light conversion properties exhibit high BSI values indicating that BSI may provide a means of phosphor performance evaluation for imaging applications.

Key words: Radiography, phosphor; screens and films; X-ray luminescence; technology.

Correspondence: Dionisis Cavouras, Department of Medical Instrumentation Technology, Technological Educational Institution of Athens, Ag. Spyridonos Street, Aigaleo, GRE-122 10 Athens, Greece. FAX +30 1 59 10 975.

Accepted for publication 24 August 1998.

In X-ray imaging, scintillators (phosphors) are used as radiation detectors of medical imaging systems. Phosphors are usually employed in the form of fluorescent layers, often called phosphor screens, deposited on or combined with a light photon detector (photocathode, photodiode, or film). X-ray image quality (1, 2, 4, 7) is largely affected by the performance of phosphors. Performance is assessed by various parameters based on the following phosphor properties: the X-ray luminescence efficiency (XLE), expressing the capability of a scintillator to emit high light inten-

sity for a given incident X-ray intensity, and the ability of a scintillator to produce images displaying small anatomic details. XLE is related to image brightness, to patient dose burden, as well as to quantum noise, which in turn affects the perceptibility of low contrast structures. The second phosphor property is related to image sharpness, spatial resolution, and contrast in relation to object dimensions, which can be estimated by measuring the edge, point, or line spread functions (ESF, PSF, LSF) or the modulation transfer function (MTF) of the imaging system.

The purpose of the present study was to propose an image quality index for assessing the quality of the image produced by phosphors used in X-ray imaging. This quality index is defined as the brightness-sharpness index (BSI) expressing both light intensity and image sharpness of medical images. Other quality indices currently in use (2, 7) require a large number of input data and/or necessitate laborious experimental techniques.

Material and Methods

Theory: The X-ray luminescence efficiency (η_Φ) of a phosphor screen is a measure of an image receptor's sensitivity expressing the brightness obtained in the final image for a given level of patient exposure. XLE is defined (11) as:

$$\eta_\Phi = \Psi_L / \Psi_X \quad (\text{Rel. 1})$$

where Ψ_L is the light intensity emitted by a screen when excited by an incident X-ray intensity Ψ_X . XLE has been equivalently defined (11) as the product of three parameters as follows:

$$\eta_\Phi = \eta_Q \eta_C G_L \quad (\text{Rel. 2})$$

where η_Q is the X-ray detection efficiency, giving the detection probability of an incident X-ray quantum, η_C is the intrinsic X-ray to light conversion efficiency, expressing the fraction of absorbed X-ray energy that is converted into light within the phosphor material, and G_L is the light transmission efficiency, giving the probability of light photon transmission and escape from the phosphor material. XLE may be considered as a brightness index comparing a real phosphor screen to an ideal screen with $\eta_{\Phi_{\text{ideal}}} = 1$. Hence $\eta_\Phi / \eta_{\Phi_{\text{ideal}}} = \eta_\Phi$.

The visibility of small anatomic details may be assessed by the modulation transfer function. MTF is a curve which expresses the transfer of contrast through the imaging system as well as the spatial resolution of an imaging system. However, to express image sharpness by a single index value instead of a spatial frequency dependent function such as the MTF, the noise equivalent passband (Ne) (4) was used. Ne is defined as the integral of the MTF squared over the spatial frequency (ω) range and is related to the quality of the image of an edge (11). Thus:

$$\text{Ne} = 2 \int_0^\infty [\text{MTF}]^2 d\omega \quad (\text{Rel. 3a})$$

Furthermore, to describe image sharpness and resolution by an index ranging from 0 to 1, Ne was divided by Ne_{ideal} corresponding to the Ne of a perfect system, i.e. a system with $\text{MTF} = 1$. Thus, the sharpness index Q was defined as:

$$Q = \frac{\text{Ne}}{\text{Ne}_{\text{ideal}}} \quad (\text{Rel. 3b})$$

The brightness - sharpness index of a phosphor screen may then be written as:

$$\text{BSI} = \eta_\Phi Q \quad (\text{Rel. 4})$$

Since both η_Φ and Q can express comparisons of real to ideal phosphor screens, BSI can also be considered as a parameter that compares the imaging performance of a real scintillator to the performance of an ideal scintillator.

Experimental procedures: BSI was experimentally determined as follows:

Screen preparation: Six test screens from each phosphor ($\text{Gd}_2\text{O}_2\text{S:Tb}$, $\text{La}_2\text{O}_2\text{S:Tb}$, and $\text{Y}_2\text{O}_2\text{S:Tb}$) were prepared following a sedimentation technique (3, 9, 10). Phosphors were in powder form with mean powder grain size of about 7 μm . A mixture of 2000 ml deionized water and 25 ml Na_2SiO_3 (binding material between grains) was employed. Screens were prepared with coating thicknesses ranging from 50 to 150 mg/cm^2 .

XLE measurements: To determine XLE (η_Φ in Rel. 4) the light intensity Ψ_L emitted by each screen (see Rel. 1) and the incident exposure rate were measured (3, 5, 10) at 50, 80, 100, and 120 kVp. The light intensity was determined by a photomultiplier (EMI 9558 QB) coupled to a Carry 401 electrometer. The exposure rate was measured by a PTW dosimeter and the exposure values were converted into X-ray intensity (energy flux) employing the appropriate exposure to X-ray energy flux conversion factor (6).

Determination of Q: MTF was measured in order to calculate Ne and Q as required by Rel. 3a and Rel. 3b, respectively. The MTF of each screen was determined according to the square wave response function (SWRF) method, explicitly described in previous studies (1, 3, 10). The phosphor screens were used in combination with a radiographic film (Agfa Curix Ortho GS), which was placed in contact with the back side of the screen. A suitable MTF test object (Nuclear Associates typ-53) comprising line pairs with spatial frequencies from 0.25 to 10 lp/mm was placed at the front side of the screen, which was irradiated by 50, 80, 100, and 120 kVp X-rays. The images of the test pattern obtained on the films (SWRF images) were digitized by a Microtec Scanmaker II SP (24 bit color 1200 \times 1200 dpi) scanner. The MTF of each phosphor screen was obtained by using Coltman's formula (1, 3, 10), which expresses the MTF in terms of the SWRF, and taking into consideration the scanner's MTF, as described in previous studies (3, 10).

Fig. 1. Variation of the brightness index (XLE) with coating thickness of $Gd_2O_2S:Tb$, $La_2O_2S:Tb$, and $Y_2O_2S:Tb$ phosphor screens measured at 80 kVp.

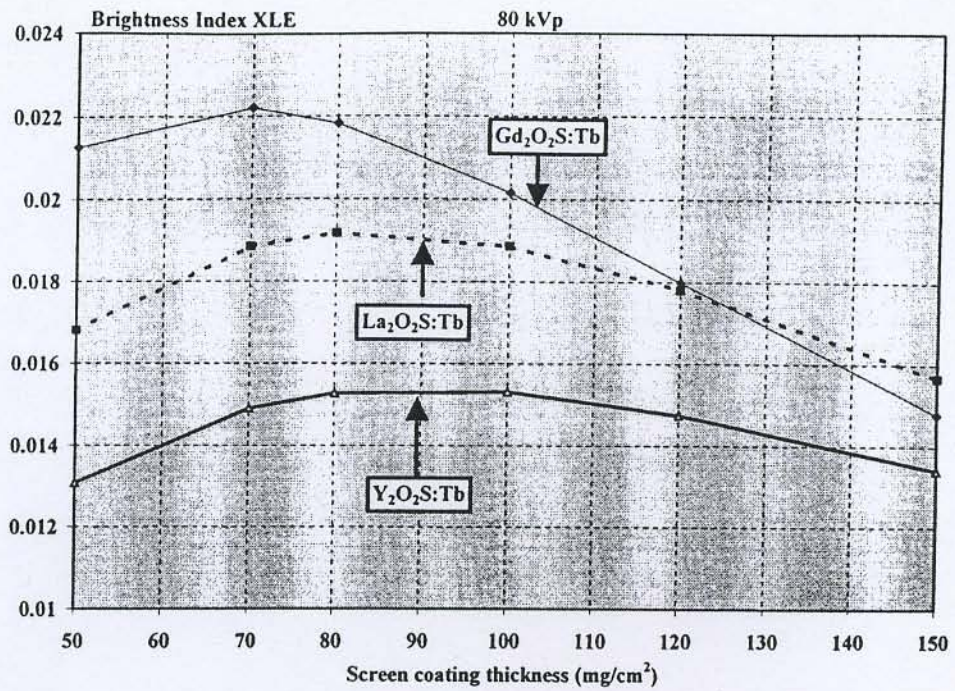
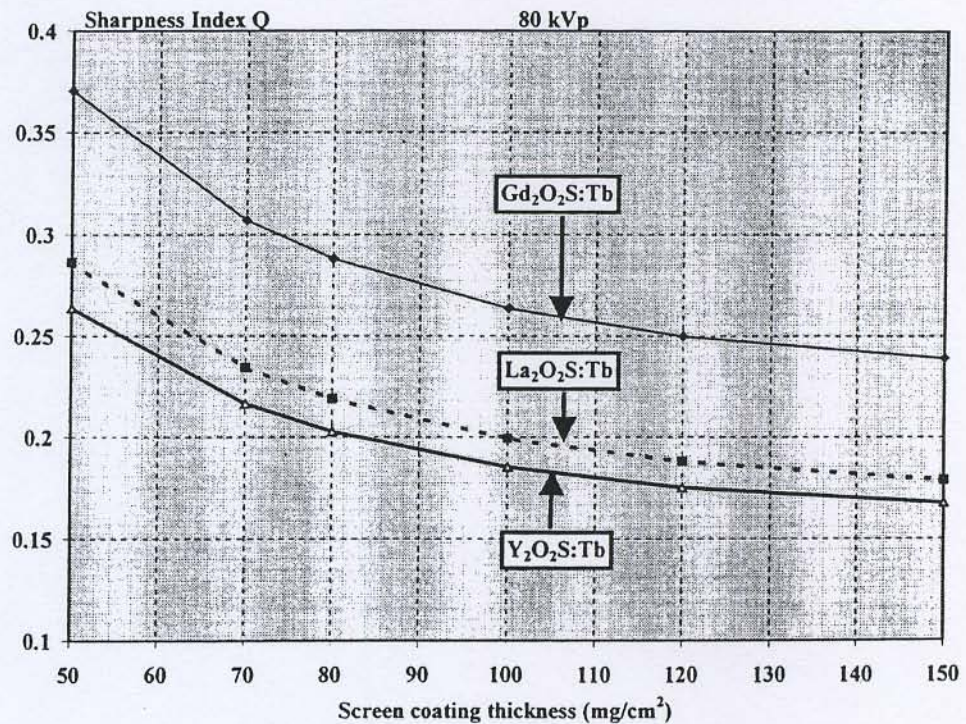


Fig. 2. Variation of the sharpness index (Q) with coating thickness of $Gd_2O_2S:Tb$, $La_2O_2S:Tb$, and $Y_2O_2S:Tb$ phosphor screens measured at 80 kVp.



Results

Fig. 1 shows the XLEs of all the screens employed in our experiments, measured at 80 kVp. $Gd_2O_2S:Tb$ exhibited higher performance than $La_2O_2S:Tb$ for screens up to 120 mg/cm^2 . On the

other hand, $La_2O_2S:Tb$ was better than $Y_2O_2S:Tb$ for all screens and better than $Gd_2O_2S:Tb$ for screens thicker than 120 mg/cm^2 .

Fig. 2 shows the variation of the sharpness index Q with increasing screen coating thickness. Q decreased rapidly up to 100 mg/cm^2 and slower there-

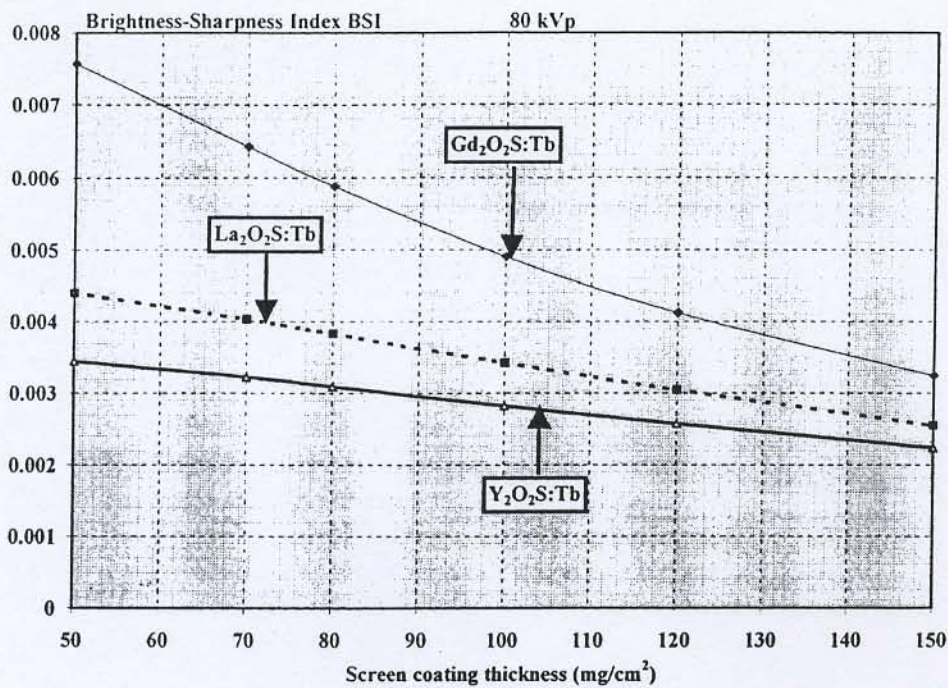


Fig. 3. Variation of the brightness-sharpness index (BSI) with coating thickness of Gd₂O₂S:Tb, La₂O₂S:Tb, and Y₂O₂S:Tb phosphor screens measured at 80 kVp.

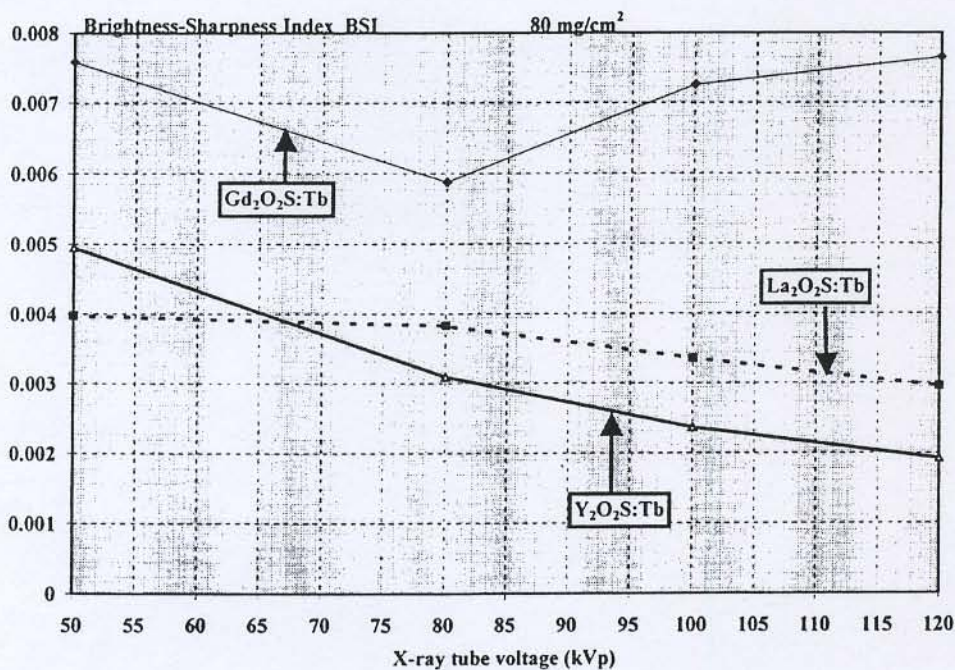


Fig. 4. Variation of the brightness-sharpness index (BSI) with X-ray tube voltage of 80 mg/cm² Gd₂O₂S:Tb, La₂O₂S:Tb, and Y₂O₂S:Tb phosphor screens.

after. The Gd₂O₂S:Tb screens performed better than screens prepared from La₂O₂S:Tb and Y₂O₂S:Tb.

The variation of the BSI with screen coating thickness at 80 kVp is presented in Fig. 3. Gd₂O₂S:Tb screens showed highest values while La₂O₂S:Tb was found better than Y₂O₂S:Tb. BSI

decreased with phosphor thickness at a rate depending on the phosphor type. For Gd₂O₂S:Tb the decrease rate was very rapid as compared to other phosphors.

Fig. 4 shows the variation of BSI with X-ray tube voltage for the 80 mg/cm² phosphor screens. The BSI of Gd₂O₂S:Tb showed a minimum value

at 80 kVp, while the BSIs of the other phosphors were continuously decreasing.

Discussion

The variation of XLE (brightness index) with screen coating thickness, shown in Fig. 1, is governed by the variation of the X-ray detection efficiency (η_Q) and the light transmission efficiency (G_L) (see Rel. 2). X-ray detection efficiency of a phosphor screen initially increases with screen coating thickness but gradually obtains a constant value. On the other hand, G_L has a tendency to decrease with phosphor thickness, since the probability of light scattering or absorption is higher for thick screens. Thus, in the case of thin screens, the XLE curves are increasing, mainly affected by η_Q , while for screens of medium to high coating weight, the curves are decreasing due to the influence of G_L . $Gd_2O_2S:Tb$ was found the most luminescent phosphor. This may be explained by the high density (7.34 g/cm^3), high effective atomic number ($Z(Gd)=64$), and high intrinsic conversion efficiency ($\eta_C=0.2$) of $Gd_2O_2S:Tb$ (8). These properties augment the importance of X-ray absorption and X-ray-to-light conversion processes, resulting in higher light output. However, for screen thickness larger than 125 mg/cm^2 , the $La_2O_2S:Tb$ screens performed better. This may be explained by the deeper penetration of X-rays in $La_2O_2S:Tb$ than in $Gd_2O_2S:Tb$, because of the lower density and atomic number of $La_2O_2S:Tb$. For thick screens, X-rays will be totally absorbed deeper in the $La_2O_2S:Tb$ phosphor screen mass and, thus, closer to the emitting back side of the screen. This results in lower light attenuation and higher XLE.

The variation of sharpness index Q with coating thickness in Fig. 2 may be explained by considering that light spreads to a greater extent as screen thickness increases. This results in a PSF broadening giving lower values of MTF and Q . However, for thicker screens the probability of optical absorption increases for the laterally directed optical photons, since they have to travel longer distances to escape the screen. Thus, only the central part of the optical trajectories contributes to the light output and this reduces the rate of PSF broadening for screens thicker than 100 mg/cm^2 . The superiority of $Gd_2O_2S:Tb$ sharpness index in Fig. 2 is due to better MTF because $Gd_2O_2S:Tb$ was the most luminescent phosphor, giving high intensity depiction of the lead-bars test-pattern spaces and, thus, high contrast SWRF images and high MTF values. The material density of $Gd_2O_2S:Tb$ is higher than those of $La_2O_2S:Tb$ and $Y_2O_2S:Tb$ and, thus, for equal coating thicknesses,

$Gd_2O_2S:Tb$ screens are thinner. Hence, light spread is reduced due to isotropic light propagation and scattering within the screen material, resulting in narrow PSF and better MTF values. Similar reasoning holds for MTF differences between $La_2O_2S:Tb$ and $Y_2O_2S:Tb$.

Concerning the variation of BSI with coating thickness in Fig. 3, it is interesting to note that although thick phosphor screens, due to higher η_Q , are capable of capturing a larger fraction of the incoming information carried by the incident beam, they produce images of lower BSI. This behavior may be explained by the decrease in MTF with coating thickness and by the decrease in XLE which shows a tendency to decrease at high phosphor coatings (see Fig. 1).

The ascending part of the $Gd_2O_2S:Tb$ curve in Fig. 4, starting at 80 kVp, could be explained by considering that the minimum of the X-ray absorption appears at energies just below 50 keV, which is the K-absorption edge of gadolinium (50.2 keV). The 50 keV energy should approximately correspond to the mean energy of an 80 kVp X-ray spectrum. Similarly, the flat region of the $La_2O_2S:Tb$ curve between 50 and 80 kVp should be due to the influence of the K-absorption effect of La appearing at 39 keV. The energy of the $Y_2O_2S:Tb$ K-edge (17 keV) is lower than the X-ray energies of our measurements and, hence, it does not affect the shape of the $Y_2O_2S:Tb$ curve. Thus, the BSI of $Y_2O_2S:Tb$ becomes higher than $La_2O_2S:Tb$ for tube voltages between 50 and 65 kVp.

In conclusion, BSI data showed that thin phosphor screens prepared from high density, high atomic number, and high intrinsic conversion efficiency (η_C) materials constitute image receptors with very good combination of brightness, sharpness and resolution. BSI may be employed for selecting best combinations of phosphor type, thickness, and X-ray tube voltage. It is, thus, applicable to many types of X-ray image detectors including the recently introduced flat panel detectors for digital radiography, which consist of a CsI:Tl phosphor coupled to an amorphous silicon light photon detector (12).

ACKNOWLEDGMENT

This study is dedicated to the memory of Prof. G. E. Giakoumakis, leading member of our team, whose work on phosphor materials has inspired us to continue this research.

REFERENCES

1. BARNES G. T.: The use of bar pattern test objects in assessing the resolution of film/screen systems. *In*: The phys-

- ics of medical imaging recording system measurements and techniques, p. 138. Edited by A. G. Haus. American Association of Physicists in Medicine, New York 1979.
2. BUNCH P. C., HUFF K. E. & VAN METTER R.: Analysis of the detective quantum efficiency of radiographic film-screen combination. *J. Opt. Soc. Am. A4* (1987), 902.
 3. CAVOURAS D., KANDARAKIS I., PANAYOTAKIS G., EVANGELOU E. K. & NOMICOS C. D. An evaluation of the $Y_2O_3:Eu^{3+}$ scintillator for application in medical X-ray detectors and image receptors. *Med. Phys.* 23 (1996), 1965.
 4. EVANS A. L.: The evaluation of medical images, p. 45. Adam Hilger Ltd., Bristol 1981.
 5. GIAKOUMAKIS G. E., NOMICOS C. D., SKOUNTZOS P. et al.: $Y_2O_2S:Eu$ phosphor screens evaluation. *Med. Phys.* 20 (1993), 79.
 6. HENDEE W. R.: Medical radiation physics, p. 145. Year Book Medical Publishers, Chicago 1970.
 7. KANAMORI H. & MATSUOTO M.: The information spectrum as a measure of radiographic image quality and system performance. *Phys. Med. Biol.* 29 (1984), 303.
 8. KANDARAKIS I., CAVOURAS D., PANAYOTAKIS G., AGELIS T., NOMICOS C. & GIAKOUMAKIS G.: X-ray induced luminescence and spatial resolution of $La_2O_2S:Tb$ phosphor screens. *Phys. Med. Biol.* 41 (1996), 297.
 9. KANDARAKIS I., CAVOURAS D., PANAYOTAKIS G. S. & NOMICOS C.: Evaluating X-ray detectors for radiographic applications. A comparison of $ZnSCdS:Ag$ with $Gd_2O_2S:Tb$ and $Y_2O_2S:Tb$ screens. *Phys. Med. Biol.* 42 (1997), 1351.
 10. KANDARAKIS I., CAVOURAS D., PANAYOTAKIS G. S., TRIANTIS D. & NOMICOS C. D.: An experimental method for the determination of spatial frequency dependent detective quantum efficiency (DQE) of scintillators used in X-ray imaging detectors. *Nucl. Instr. Meth. Phys. Res. A* 399 (1997), 335.
 11. LUDWIG G. W.: X-ray efficiency of powder phosphors. *J. Electrochem. Soc.* 118 (1971), 1152.
 12. SPAHN M., ALEXANDER J. & GMEINWIESER J.: Amorphous silicon solid-state detectors and their future application in medical X-ray imaging. *Electromedica* 65 (1997), 37.